High-field transport properties of $InAs_xP_{1-x}$/InP ($0.3 \leqslant x \leqslant 1.0$) modulation doped heterostructures at 300 and 77 K

D. Yang and P. K. Bhattacharya
Solid State Electronics Laboratory, Department of Electrical Engineering & Computer Science, The University of Michigan, Ann Arbor, Michigan 48109-2122

W. P. Hong, R. Bhat, and J. R. Hayes
Bellcore, 331 Newman Springs Road, Red Bank, New Jersey 07701

(Received 16 December 1991; accepted for publication 16 March 1992)

We have measured the high-field transport characteristics of pseudomorphic $InAs_xP_{1-x}$/InP ($0.3 \leqslant x \leqslant 1.0$) modulation doped heterostructures at 300 and 77 K. The field dependent steady state average velocities increase steadily with increase in x. The maximum velocities that have been measured in InAs/InP are 1.7×10^7 cm/s (2.5 kV/cm) and 3.2×10^7 cm/s (2.2 kV/cm) at 300 and 77 K, respectively. These are the highest velocities measured in any modulation doped heterostructure. The field dependent channel carrier concentration and mobility data indicate that there is very little real space transfer of carriers at high fields and this is confirmed by results from steady state Monte Carlo calculations.

I. INTRODUCTION

The InAsP/InP strained heterostructure system is potentially useful for long-wavelength optoelectronic device applications.[1-3] It can also be a heterostructure of choice for high-performance heterostructure field effect transistors. Recent theoretical work has predicted their suitability for short channel devices.[4] Experimental work on relaxed InAsP alloys[5] indicates that the transport properties are very favorable and the Γ-L separation is quite large (Table I). We have recently made[6] 0.5 μm gate modulation doped field effect-transistors (MODFETs) with pseudomorphic $InAs_{0.6}P_{0.4}$/InP heterostructures and the results are very promising. The measured value of the maximum external transconductance is 320 mS/mm and f_T and f_{max} in the same device are 55 and 60 GHz, respectively. In this work we have made a systematic study of the high field transport parameters—electron velocity and mobility—in pseudomorphic $InAs_xP_{1-x}$/InP ($0.3 \leqslant x \leqslant 1.0$) heterostructures.

II. EXPERIMENTAL TECHNIQUES

The $InAs_xP_{1-x}$/InP modulation doped heterostructures were grown in a low-pressure (76 Torr) organometallic chemical vapor deposition (OMCVD) reactor. The epitaxial layer structures are shown in Fig. 1(a). Reagents were trimethylindium (TMI), 10% arsine in hydrogen, and 20% phosphine in hydrogen. Hydrogen sulfide diluted to 1000 ppm in hydrogen was used as an n-type dopant source. The doping level of the doped InP layer is 3×10^{18} cm^{-3}. The mole fraction of TMI was set at 4.375×10^{-5} to give a growth rate of about 6.8 Å/s. As the strain increases there is an increasing tendency for balling-up and hence three-dimensional growth. This tendency is enhanced by the high mobility of the indium on the growing surface. In order to overcome this problem, high total group V mole fraction and low growth temperature were used with the temperature decreasing as the strain increased. The thickness of the $InAs_xP_{1-x}$ channel layer (y) was 100 Å for $x=0.3$, 0.6, and 0.8, whereas it was reduced to 50 Å for $x=1.0$. For comparison, a lattice matched $In_{0.53}Ga_{0.47}As$/InP heterostructure, indicated in Fig. 1(a), was also grown. Some measured parameters of the layers are listed in Table I.

The compositions of the layers were measured by using double crystal x-ray diffraction and were determined by matching experimental x-ray rocking curves of the structures shown in Fig. 1(a) to those of simulations from the dynamical x-ray diffraction theory.[7] The effect of strain on the lattice parameters was included in the simulation.

Velocity-field and mobility-field characteristics were made on planar H devices[8] and Hall bar geometry devices. These devices were fabricated using a planar process. First, mesa isolation was made by a 0.2–0.25 μm wet chemical etch. Ohmic contacts were made by electron-beam evaporation of Ge/Au/Ni/Ti/Au followed by rapid thermal annealing. The schematic of the H device, shown in detail in Ref. 8, is shown in Fig. 1(b), where the dimensions are also indicated. The electric field is determined from the potential profile in the bridge region measured at successive ohmic contact fingers along the bridge, which are not shown. This particular device geometry ensures that possible domains nucleating near the contacts will not propagate into the bridge region and interfere with the measurement when time current instabilities occur. The input voltage pulse (200 ns) and output current pulse are recorded on a sampling scope. The carrier velocity is computed from the measured current density by taking into account the field dependent carrier density obtained from pulsed field dependent Hall measurements. All the measured results indicate that the electric field distribution was uniform in the bridge region.

III. RESULTS AND DISCUSSION

The velocity-field characteristics of $InAs_xP_{1-x}$/InP ($0.3 \leqslant x \leqslant 1.0$) computed from measurements at 300 K are shown in Fig. 2(a). The highest field shown for each composition represents the point beyond which accurate mea-

 0021-8979/92/130174-05$04.00

TABLE I. Transport-parameters of $InAs_xP_{1-x}$/InP and $In_{0.53}Ga_{0.47}As$/InP modulation doped heterostructures.

Modulation doped sample	$InAs_xP_{1-x}$ channel composition (x)	Channel band gap at 300 K (eV)	$E_{\Gamma-L}$ in InAsP (eV)[17]	$\Delta E_c=0.65\Delta E_g$ for InAsP/InP (eV)[18]	Hall data for $E=0$ at 300 K	
					$\eta_s\times10^{12}$ (cm^{-2})	μ ($cm^2/V\,s$)
A	0.3	1.053	0.743	0.193	1.88	3100
B	0.6	0.756	0.887	0.386	2.29	6100
C	0.8	0.558	0.982	0.515	2.39	7700
D	1.0	0.36	1.078	0.644	5.75	6900
E	$In_{0.53}Ga_{0.47}As$/InP	0.74	0.55	0.308	1.55	8500

surements were not possible due to the development of current instabilities. The cause of such instabilities could be intervalley transfer, intersubband transfer, and real space transfer into the buffer layers. For comparison, the measured room-temperature velocity-field characteristics of the lattice-matched $In_{0.53}Ga_{0.47}As$/InP modulation doped (MD) heterostructure is shown in Fig. 2(b).

Several observations can be made from the data of Figs. 2(a) and 2(b). First, the measured velocity at a field

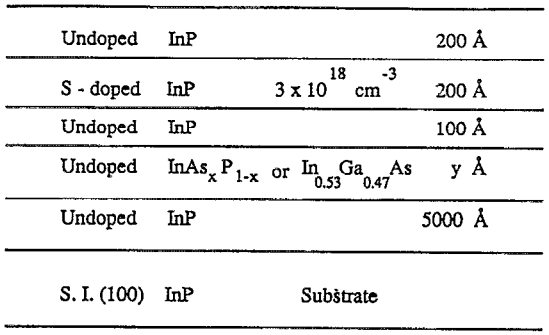

(a)

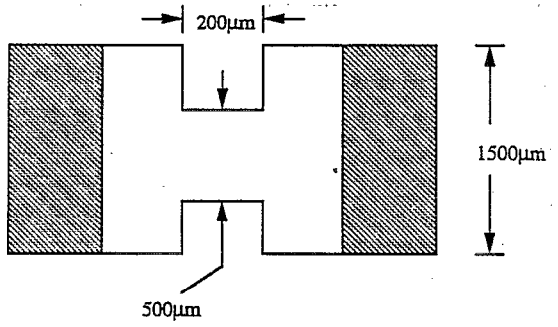

(b)

FIG. 1. (a) Schematic of $InAs_xP_{1-x}$/InP and $In_{0.53}Ga_{0.47}As$/InP modulation doped heterostructures grown by low-pressure OMCVD, and (b) schematic of H device defined by photolithography and used to measure velocity-field characteristics.

of 2 kV/cm in the $In_{0.53}Ga_{0.47}As$/InP is 1.0×10^7 cm/s, which is only slightly lower than the velocity measured at the same field in lattice-matched $In_{0.53}Ga_{0.47}As$/$In_{0.52}Al_{0.48}As$ MD heterostructures grown by molecular beam epitaxy (MBE).[8] As shown in Table I ($\Delta E_c\geq0.19$ eV for $x\geq0.3$) due to charge confinement and the difference of electron affinity between the two materials, most of the carriers will remain in the channel within the range of fields in which measurements were made. These velocities therefore represent the intrinsic transport properties of the two-dimensional electron gas in all the heterojunctions. From Fig. 2(a) it is seen that in $InAs_xP_{1-x}$/InP structures, the velocities increase steadily with field as x increases. In the range of fields over which measurements have been made, this mainly reflects the increase of the mobility $\mu(E)=\vartheta(E)/E$ with reduction in band gap and/or effective mass. It should be noted that the highest velocities that have been measured are not the peak or saturation velocities. For example, for the InAs/InP sample, the highest velocity measured at room temperature is 1.7×10^7 cm/s at a field of 2.5 kV/cm. This is the highest velocity measured in a pseudomorphic modulation doped heterostructure at room temperature[8–10] and it is clear that at a field of 3 kV/cm, or slightly beyond, the average velocity of carriers in the InAs channel could be much larger. In addition to the low gap materials being used, the quality of the materials and heterointerfaces are also probably responsible for this improvement.

We will next describe and discuss the field dependent mobility and carrier concentration data, shown in Figs. 3 and 4, respectively. In Fig. 3 it is seen that $\mu(E)$ remains unchanged until $E=700$–1000 V/cm, beyond which the mobility decreases. At zero or low fields the mobility in the two-dimensional electron gas (2 DEG) channel is limited mainly by optical phonon scattering, remote and background impurity scattering, alloy scattering, interface roughness scattering, and intersubband scattering. It is seen that for $E<700$ V/cm, the mobility values are progressively higher for x increasing from 0.3 to 0.8, and then no significant change is seen for $x=1.0$. The increase mainly reflects reduced intersubband scattering, slightly reduced effective mass, and reduced remote impurity scattering due to increasing ΔE_c.[11–13] The reason for a lack of improvement in going from $x=0.8$ to 1.0 is thought to be due to increased interface roughness resulting from a three-dimensional island growth mode[14] at high values of strain.

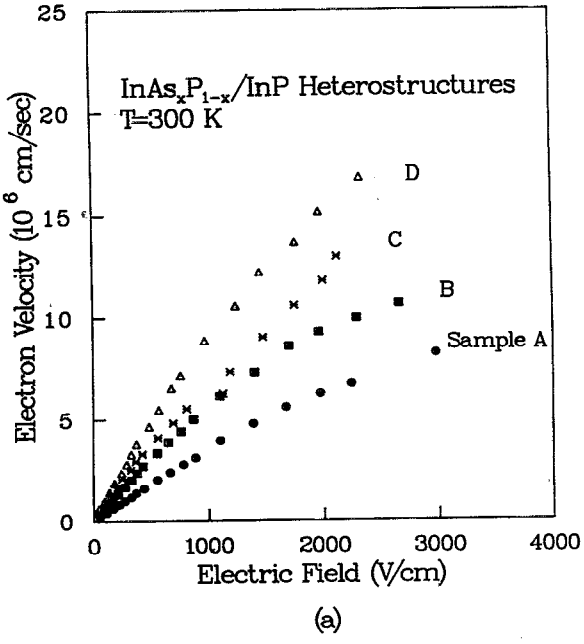

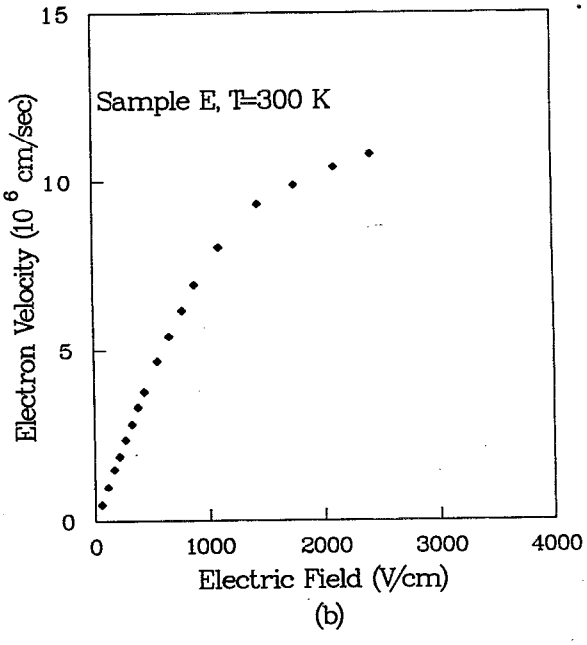

FIG. 2. Measured velocity-field characteristics of modulation doped $InAs_xP_{1-x}$/InP (a) and $In_{0.53}Ga_{0.47}As$ (b) at room temperature.

In addition, for the sample with the InAs channel, the effective mass is actually enhanced due to the stronger confinement in a thinner channel. This was confirmed by electron cyclotron resonance measurements (from $0.0497m_0$ for $x=0.8$ to $0.0567m_0$ for $x=1.0$). The decrease of mobility beyond $E=(0.8\text{–}1.0)\times10^3$ V/cm is principally due to increased phonon scattering and alloy scattering, as observed from steady state Monte Carlo analysis in the course of this work. Another minor effect may be tunneling of carriers to heterointerface defects in the InAlAs layer.[15]

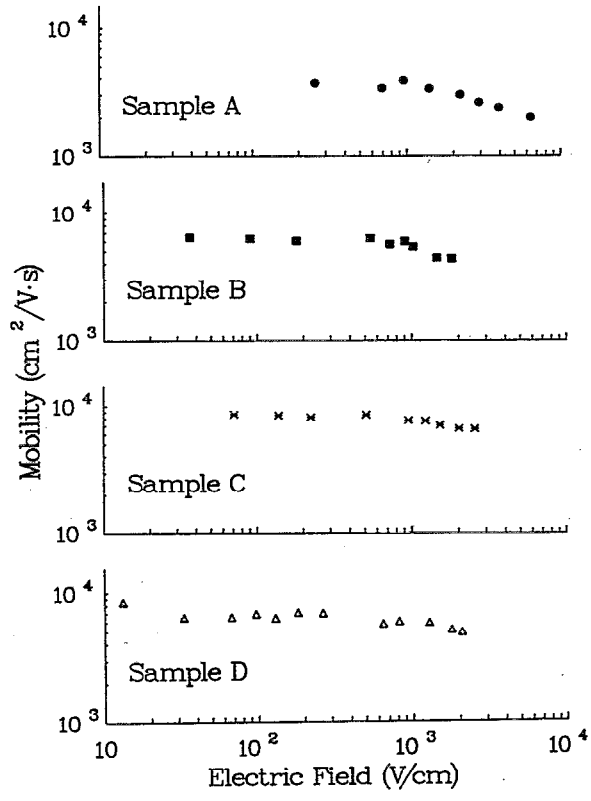

FIG. 3. Measured mobility-field characteristics of modulation doped $InAs_xP_{1-x}$/InP with $x=0.3$, 0.6, 0.8, and 1.0 at room temperature.

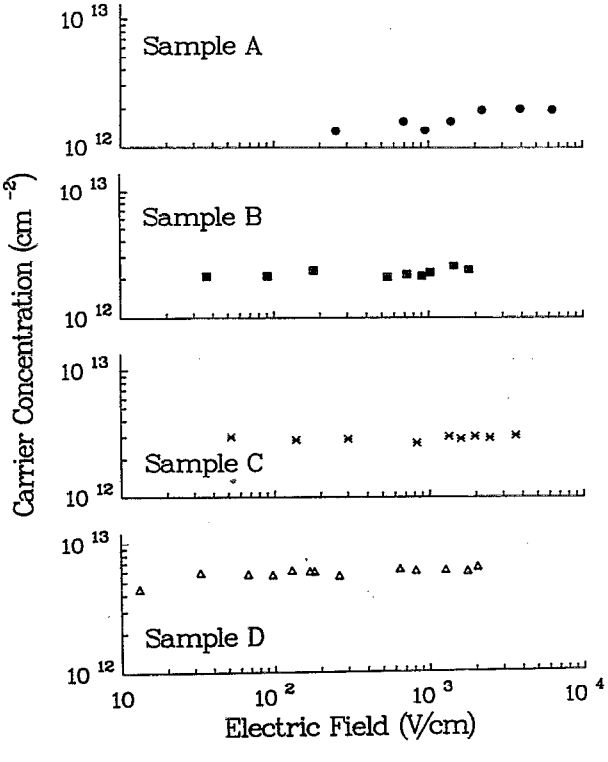

FIG. 4. Measured variation of sheet electron concentration with electric field for $InAs_xP_{1-x}$/InP modulation doped heterostructures with $x=0.3$, 0.6, 0.8, and 1.0 at room temperature.

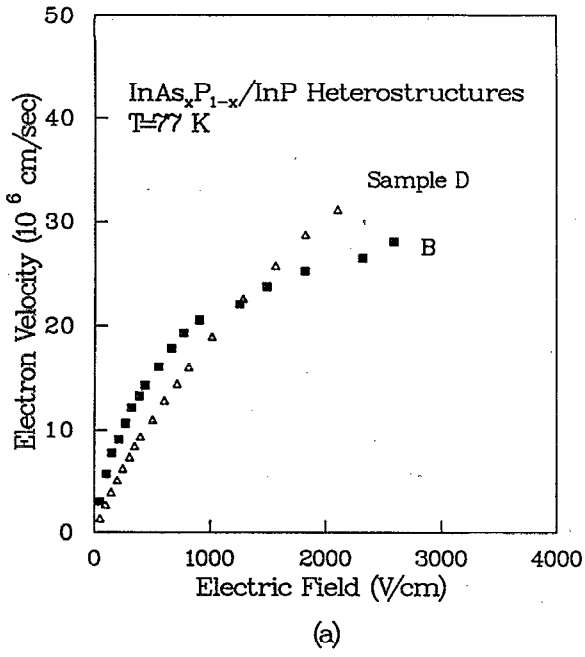

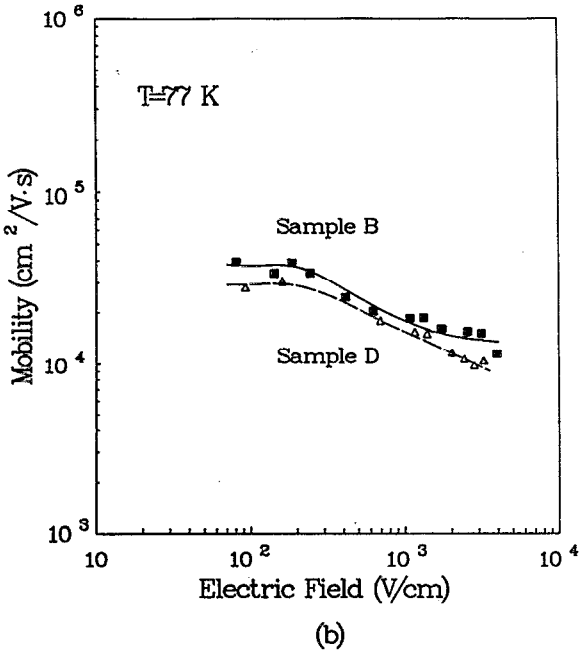

FIG. 5. (a) Velocity-field and (b) mobility-field characteristics of $InAs_xP_{1-x}/InP$ modulation doped heterostructures ($x=0.6$ and 1.0) at 77 K. The lines in (b) are joins of data.

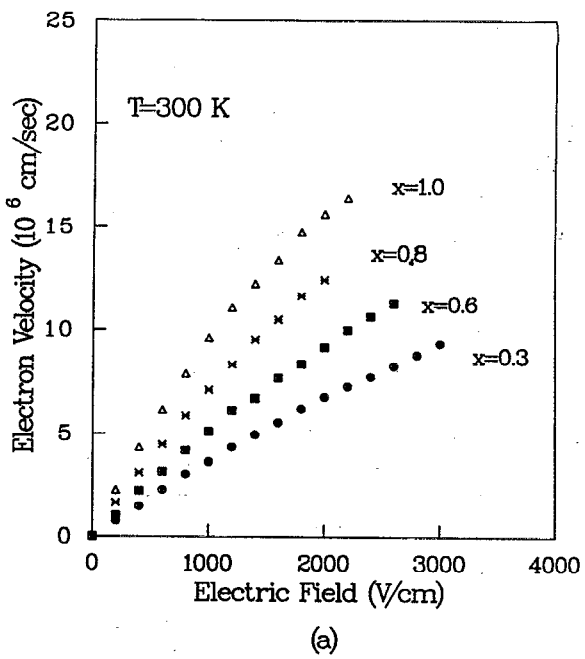

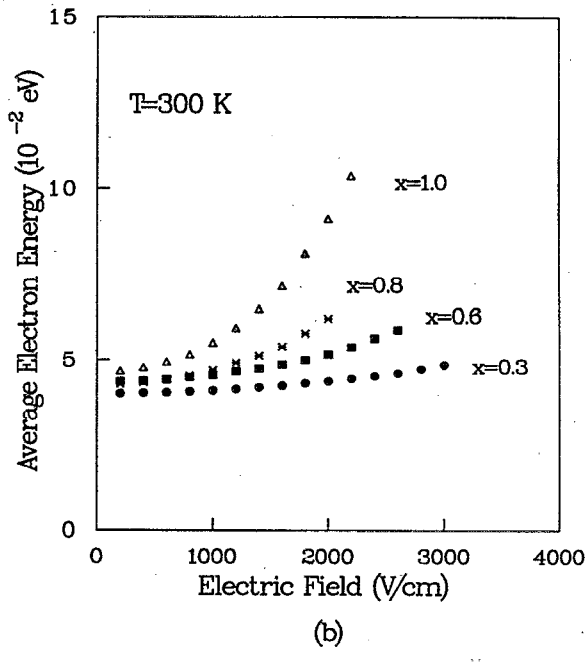

FIG. 6. (a) Velocity-field characteristics and (b) average electron energy in the channel of $InAs_xP_{1-x}/InP$ modulation doped heterostructures at 300 K obtained from steady-state Monte Carlo calculations.

It is interesting to note that the mobility decrease with an $E^{-0.35}$ dependence in $InAs_{0.3}P_{0.7}/InP$ and with an $E^{-0.3}$ dependence in $InAs_{0.6}P_{0.4}/InP$. For $x=0.8$ and 1.0, the dependence is also $E^{-0.2}$. In general, the decrease in the slope is expected due to the increasing depth of the pseudomorphic well and subsequent reduction in the probability of transfer of electrons out of the well. The fact that the slope remains unchanged for $x=0.8$ and 1.0 suggests that, phonon scattering remaining constant, there may be a relatively larger fraction of electrons leaving the channel at high fields, but not significantly larger. The spillover of some carriers into the buffer layer in the InAs/InP structure is also reflected in the relatively low measured mobility values.

The field dependent electron concentration in the different samples are depicted in Fig. 4. The concentration remains fairly constant with the field with, at best, a very small positive slope. The results suggest that there are no detrapping effects due to traps and interface states and no spurious injection of carriers from the contacts. The results

reflect, to some extent, the high quality of the heterostructures.

Finally, we will discuss the results obtained from measurements made at 77 K. The $\vartheta - E$ and $\mu - E$ data from $x=0.6$ and 1.0 are shown in Figs. 5(a) and 5(b), respectively. The maximum velocity measured in the InAs sample ($>3\times10^7$ cm/s) is higher than that measured in any other MD heterostructures at 77 K at a comparable electric field. It may be noted in Fig. 5(a) that at low field the velocities and mobilities (slope of the $\vartheta - E$ curve) are higher in the $In_{0.6}As_{0.4}P$ channel than in the InAs channel. This is contrary to expectation and can only be accounted for by a higher degree of interface roughness in the latter due to the island mode of growth. At high fields, higher velocities are measured in the InAs channel than in the $InAs_{0.6}P_{0.4}$ channel. This is due to an increase in the field dependent alloy scattering in the $InAs_{0.6}P_{0.4}$ channel. The corresponding mobility field data are shown in Fig. 5(b).

With the assumption that at low fields, for which real space transfer is insignificant, the transport properties in a bulk channel and a 2-DEG are similar,[16] a steady state Monte Carlo analysis was performed for bulk $InAs_xP_{1-x}$ ($0.3\leqslant x\leqslant 1.0$) materials at 300 K. The InAsP material parameters used in this calculation are obtained from interpolating over binary systems.[17] Only Γ and L valleys are considered in this analysis. The scattering mechanisms considered include polar optical phonon scattering, acoustic phonon scattering, intervalley scattering, ionized impurity scattering, and alloy scattering. The average electron drift velocity and electron energy are calculated at a field strength of 0–3000 V/cm. The calculated drift velocities for different As compositions are shown in Fig. 6(a). The calculated velocities agree remarkably well with the measured values in Fig. 2(a). The calculated electron energies are shown in Fig. 6(b). The electron energy remains almost constant for the range of the electric fields except for InAs in which the electron energy increases abruptly at fields greater than 1000 V/cm. Even at the highest field the average electron energy is 0.1 eV. This may be compared with the Γ-L separation of 1.08 eV in InAs[18] and $\Delta E_c = 0.644$ eV in the InAsP/InP heterostructure (assuming $\Delta E_c = 0.65\ \Delta E_g$, which may not be strictly true). Therefore, most of the carriers in InAs/InP remain in the channel at the fields applied during these measurements. However, it is important to realize that in a practical $InAs_xP_{1-x}$/InP MD heterostructure where x is large, the electron effective mass is small, and the channel thickness is also kept small. Therefore, a significant fraction of the carrier wave function may reside in regions outside the channel. Under such conditions the transport properties of the regions outside the channel will become important in determining the device performance.

IV. CONCLUSION

In conclusion, we have made detailed measurements at 300 and 77 K of the high-field transport properties of pseudomorphic InAsP/InP modulation doped heterostructures grown by low-pressure OMCVD. Two significant results emerge from our measurements. First, the high-field channel velocities are comparable to or better than that of InGaAs/InAlAs heterostructures. Second, the transport properties of InAs/InP heterostructures suggest that carriers remain confined in the channel even at high fields. The results clearly demonstrate the potential of this heterostructure for the design of high performance MODFETs and work in this area is already under way in our group.

ACKNOWLEDGMENT

The work at the University of Michigan is supported by NASA-Lewis Research Center under Grant NAG-3-988.

[1] R. P. Schneider, Jr., D. X. Li, and B. W. Wessels, J. Electrochem. Soc. **136** 3491 (1989).
[2] T. K. Woodward, T. Sizer, and T. H. Chu, Appl. Phys. Lett. **58** 1366 (1991).
[3] H. Q. Hou, C. W. Tu, and S. N. G. Chu, Appl. Phys. Lett. **58**, 2954 (1991).
[4] S. Krishnamurthy, A. Sher, and A.-B. Chen, Appl. Phys. Lett. **52**, 468 (1988).
[5] A. El-Sabbathy, A. R. Adams, and M. L. Young, Solid State Electron. **21**, 83 (1978).
[6] W.-P. Hong, J. R. Hayes, R. Bhat, P. S. D. Lin, C. Nguyen, H. P. Lee, D. Yang, and P. K. Bhattacharya, presented at the International Electron Devices Meeting, Washington, DC, December 1991.
[7] P. J. Burgeat and D. Taupin, Acta Crystallogr A **24**, 99 (1968).
[8] W.-P. Hong and P. K. Bhattacharya, IEEE Trans. Electron Devices **ED-34**, 1491 (1987).
[9] N. Shigekawa, T. Furtua, and K. Arai, J. Appl. Phys. **69**, 4003 (1991).
[10] S. Sasa, Y. Nakata, T. Fujii, and S. Hiyamizu, in *Proceedings of the International Symposium on GaAs and Related Compounds*, Heraklion, Greece, edited by A. Christou and H. S. Rupprecht (Institute of Physics, Bristol, 1988), pp. 407–410.
[11] W.-P. Hong, G. I. Ng, P. K. Bhattacharya, D. Pavlidis, S. Willing, and B. Das, J. Appl. Phys. **64**, 1945 (1988).
[12] A. Kastalsky, R. Dingle, K. Chang, and A. Y. Cho, Appl. Phys. Lett. **41**, 274 (1982).
[13] S. Mori and T. Ando, J. Phys. Soc. Jpn. **48**, 865 (1980).
[14] Y. C. Chen, P. K. Bhattacharya, and J. Singh, J. Cryst. Growth **111**, 228 (1991).
[15] W.-P. Hong, J. E. Oh, P. Bhattacharya, and T. Tiwald, IEEE Trans. Electron. Dev. **35**, 1585 (1988).
[16] K. F. Brennan and D. H. Parks, J. Appl. Phys. **65**, 1156 (1989).
[17] S. Adachi, J. Appl. Phys. **53**, 8775 (1982).
[18] M. V. Fischetti, IEEE Trans. Electron Devices **38**, 634 (1991).